Microporous and Mesoporous Materials 270 (2018) 34–39

Contents lists available at ScienceDirect

Microporous and Mesoporous Materials

journal homepage: www.elsevier.com/locate/micromeso

Prolonged HKUST-1 functionality under extreme hydrothermal conditions by electrospinning polystyrene fibers as a new coating method

Mitchell Armstrong[a], Peyman Sirous[a], Bohan Shan[a], Ruitong Wang[b], Congwei Zhong[b], Jichang Liu[b,**], Bin Mu[a,*]

[a] Chemical Engineering, School for Engineering of Matter, Transport, and Energy, Arizona State University, 501 East Tyler Mall, Tempe, AZ 85287, USA
[b] State Key Laboratory of Chemical Engineering, East China University of Science and Technology, Shanghai 200237, China

ARTICLE INFO

Keywords:
Metal-organic-frameworks (MOFs)
Electrospinning
Water stability
HKUST-1
Core-shell adsorbents

ABSTRACT

The metal-organic framework (MOF) HKUST-1 (CuBTC) has been regarded as a promising adsorbent due to its open metal sites, easy synthesis method, and lower synthesis cost. However, a big challenge related to its practical application is its poor hydrostability. The porosity of as-synthesized HKUST-1powder may drop 50% in less than one month and it can decompose within days at high humid and hot atmosphere. In this work, we demonstrate that the hydrothermal stability of HKUST-1 is greatly improved after coating it with a thin hydrophobic polymer. The HKUST-1 particles may be directly impregnated in polystyrene fibers during the electrospinning process by suspending sonochemically synthesized HKUST-1 powder in the polystyrene dope solution. It was confirmed that the final HKUST-1 loading was 5% by TGA. Nitrogen isotherms do not show the expected nitrogen uptake in these fibers; however, the carbon dioxide isotherms do. This suggests that the particles are embedded under a layer of polystyrene in agreement with SEM images, and that the nitrogen is unable to penetrate this layer over the length of a nitrogen adsorption experiment. HKUST-1 powder and 5 wt% HKUST-1 fibers are exposed to extreme hydrothermal conditions, and CO_2 uptake is measured at varying time steps. Nearly complete hydrolytic degradation of pure HKUST-1 powder is observed at 6 h, but the rate of degradation in the 5 wt% HKUST-1 impregnated fibers is slowed, and 20% CO_2 uptake capacity is still observed at 48 h.

1. Introduction

Incorporating open metal sites into metal-organic frameworks (MOFs) leads to elevated functionality in terms of uptake capacity. These open metal sites provide leading properties for hydrogen storage [1], carbon dioxide capture [2], and methane storage [3] among porous materials. Even though MOFs with open metal sites (OMS), also called unsaturated metal sites (UMS), have flashed potential over a broad array of applications including gas storage and separation, they have yet to be used industrially.

Among other factors, the stability and cost of MOFs prohibit these materials from implementation in commercial applications [4]. A link between these issues and the high functionality of MOFs are rooted in the coordination chemistry gluing MOFs together, a *functionality-stability-cost nexus*. This is because uncovering or strengthening open-metal binding sites that are also responsible for holding the framework together comes with a tradeoff in stability. These open sites catalyze a hydrolysis reaction that results in water entering the framework and breaking apart the metal-to-linker bonds [5]. This tradeoff has been well-documented for the removal of linkers in UiO-66 to uncover OMS [6], metal-exchange to less-reactive species [7], partial blockage of open-metal sites [8], and the conclusion that increasing inertness of the metal-node increases hydrostability [9]. Strategies to overcome this tradeoff by modifying the MOF structure include linker exchanges [10], complex ligand designs [11], coatings [12], and thermal treatment [13]. Each of these strategies incorporates either multiple synthesis steps or complex ligands that ultimately induce extra costs that appear to be too expensive for an industrial scale.

Desantis and coworkers performed a techno-economic analysis on industrial MOF synthesis [14]. They provide two hypothetical synthesis routes that are projected to reach the economic goal of $10/kg MOF set by the Department of Energy for some MOFs (Fig. 1). Their projections show that Mg_2(dobdc), a MOF with cheap ligands that may be synthesized in one step, could reach costs as low as $8.25/kg. This leaves

* Corresponding author.
** Corresponding author.
E-mail addresses: liujc@ecust.edu.cn (J. Liu), bmu@asu.edu (B. Mu).

https://doi.org/10.1016/j.micromeso.2018.05.004
Received 16 January 2018; Received in revised form 26 April 2018; Accepted 2 May 2018
Available online 04 May 2018
1387-1811/

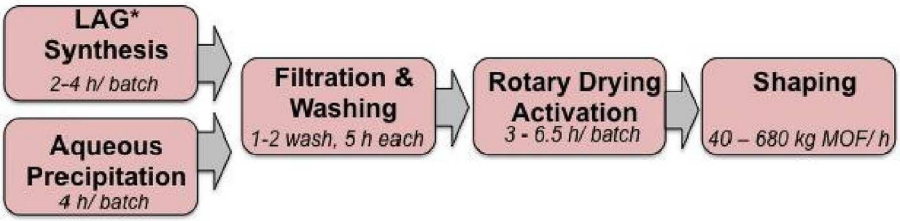

Fig. 1. Two economically viable MOF kilogram-scale synthesis procedures proposed by Desantis and coworkers. LAG stands for liquid-assisted grinding attrition mill.

little budget leftover for extra synthesis steps (with costs driven by both solvent and processing) or expensive ligands; which are two most economically sensitive expenses in the process. An alternate stage that may be exploited to address the functionality-stability-cost nexus is the shaping stage, where MOF powder is typically embedded in a highly permeable polymer substrate to form a process-ready material. Selecting a complementary polymer coating for the MOFs with OMS that attenuates water permeation could solve the stability issues of this class of MOFs, while allowing them to maintain their high functionality, while minimizing additional process expenses. To properly add both functionality and provide a process-ready composite, the shaping stage must result in a material that has both nano-scopic dimensions (mitigating resistance to gas uptake) while also properly supply macroscopic dimensions (to allow handling and implementation into a separation unit). In a previous work, we have demonstrated that electrospun fibers are able to handle both of these tasks [15]. Furthermore, work by Pimentel and coworkers demonstrated that MOF-containing fibers offer many benefits as a final shaped material including low pressure drop and high thermal heat transfer rates [16,17].

In this work we demonstrate that MOF embedded electrospun fibers may be used to prevent hydroscopic degradation of MOFs with open metal sites. We use the MOF named HKUST-1 as a characteristic MOF with open-metal sites. HKUST-1 is well-documented to have high capacities for methane and carbon dioxide [3]. It is also known undergo an irreversible hydrolysis reaction in the presence of humidity that degrades the framework over time [5]. Fig. 2 illustrates the structure of this MOF using crystallographic data from Mustafa and coworkers [18].

HKUST-1 is embedded in polystyrene fibers near a 5% loading by mass for added hydrolytic protection. Polystyrene was selected because it has shown protective properties when coating HKUST-1 from water previously through a microcapusule technique [19]. A low loading was selected for this work to ensure that the MOF in the fibers was dilute enough to be entirely wrapped by polystyrene, since excessive loadings have shown to force MOF particles to the surface of fibers and into an unprotected state in previous work [15].

From this work we see that when HKUST-1 is electrospun in polystyrene fibers that they are nearly all embedded inside the fiber, and that from SEM images the polymeric film covering the HKUST-1 particles is near 500 nm. Hydrothermal stability tests are performed on HKUST-1 powder and HKUST-1 embedded fibers showing that hydrolysis of HKUST-1 when embedded in fibers is much slower than the pure HKUST-1 powder alone.

2. Experimental

2.1. Materials synthesis

HKUST-1 was synthesized via a sonochemical route reported previously [20]. Three different fiber samples were made. Fine pure polystyrene (PS, Sigma-Aldrich, M_W = 250,000 g/mol) fibers were made from a solution of 2g PS in 10 mL dichloromethane (DCM, 99.5%, Sigma-Aldrich). Coarse pure PS fibers were made from a solution of 3g PS in 10 mL DCM. HKUST-1 embedded PS fibers were made from a solution of 2g PS with 200 mg suspended HKUST-1 in 10 mL DCM. Each solution was spun in an electrospinning apparatus described previously [20–24], at a working distance of 20 cm, a flow rate of 0.5 mL/min, and under a DC voltage of 15 kV. All samples were kept under vacuum at 100 °C overnight for activation. Digital images of the HKUST-1 powder and HKUST-1 embedded polystyrene fibers used in this study are shown in Fig. 3.

2.2. Characterization techniques

Adsorption experiments were performed on a Micrometrics Tristar II volumetric sorption apparatus. Nitrogen (N_2, ultrahigh purity, Praxair) isotherms were measured at 77K by immersion in a liquid nitrogen bath. Carbon dioxide (CO_2, ultrahigh purity, Praxair) isotherms were collected at 273 K by immersion in ice slurry. Void volume was measured with helium (ultrahigh purity, Praxair) before each run.

Scanning electron microscopy (SEM) was performed on samples with a Zeiss Evo MA10 microscope at an accelerating voltage of 15 kV. Thermal gravimetric analysis (TGA) was performed on an TA TGA Q500 instrument at a 10 °C ramp rate from 50 °C to 500 °C with N_2 gas flowing at 40 mL/min.

To analyze the hydrolysis rate of samples they are loaded into 50 mL Teflon-lined autoclaves on a raised platform over 10 mL of de-ionized water and placed in an oven at 100 °C for specified times. The HKUST-1 powder and HKUST-1 embedded fiber samples are always tested side-by-side for each given time step.

3. Results and discussion

Each of the synthesized samples are shown in Fig. 4. The SEM images show that HKUST-1 has regular facets and an average crystal diameter of nearly 3 µm, which matches previous work [20]. The

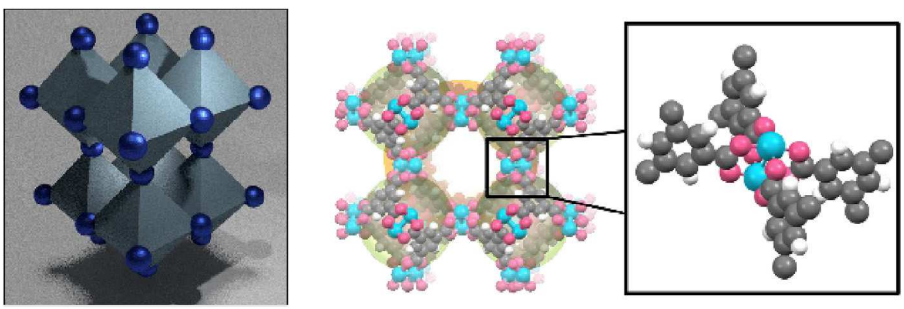

Fig. 2. Geometric representation of HKUST-1 composed of octahedron small-pore clusters and spherical metal nodes (left). Atomic model of HKUST-1 composed of carbon (grey), copper (blue), oxygen (red), and hydrogen (white) (middle). A segment of HKUST-1 demonstrating the paddle-wheel copper secondary building unit and coordinated trimesic acid ligands depicting two open-metal sites per metal cluster (right). The HKUST-1 crystal structure was provided by Mustafa and coworkers in the Cambridge Crystallographic Data Centre [18]. (For interpretation of the references to colour in this figure legend, the reader is referred to the Web version of this article.)

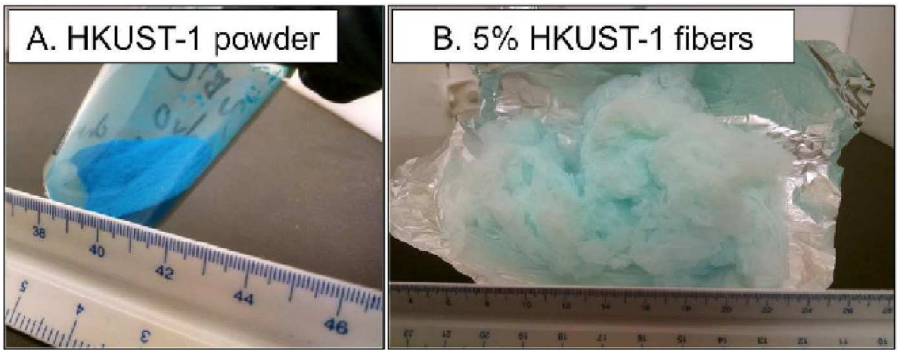

Fig. 3. Images of (A) as-synthesized HKUST-1 powder and (B) HKUST-1 embedded polystyrene fibers.

HKUST-1 embedded polystyrene fibers show that the fibers stretch to encapsulate the individual HKUST-1 particles, which is in agreement with literature [15]. From Fig. 4 (C–E) it may be observed that the coating over the particles is around 500 nm. The pure polystyrene fibers each have different diameters. The pure PS fibers in Fig. 4 (F) are called coarse fibers since they have a much larger average fiber diameter than the pure PS fibers in Fig. 4 (G)- which are called fine PS fibers.

To confirm the loading of HKUST-1 in the polystyrene fibers thermal-gravimetric analysis (TGA) was run (Fig. 5). Polystyrene burns to 1.5% of its original mass, HKUST-1 burns to 45% of its original mass, and therefore through interpolation it is approximated that the HKUST-1 embedded fibers have an HKUST-1 loading of 5 wt% since the final mass after burning is 3.5%.

N_2 isotherms were taken at 77 K and CO_2 isotherm were taken at 273 K on pure HKUST-1 powder, HKUST-1 embedded polystyrene fibers, and the two different polystyrene fiber samples. These samples are shown in Fig. 6. The resulting BET surface areas from the N_2 isotherms for these materials are 583 m^2/g for pure HKUST-1 powder, 5 m^2/g for the HKUST-1 impregnated fibers, 2.3 m^2/g for the fine PS fibers, and 0.6 m^2/g for the coarse PS fibers. The fact that the surface area of the 5% HKUST-1 fibers are < 1% of the pure HKUST-1 powder, it is expected that nearly all HKUST-1 particles are embedded under a film of

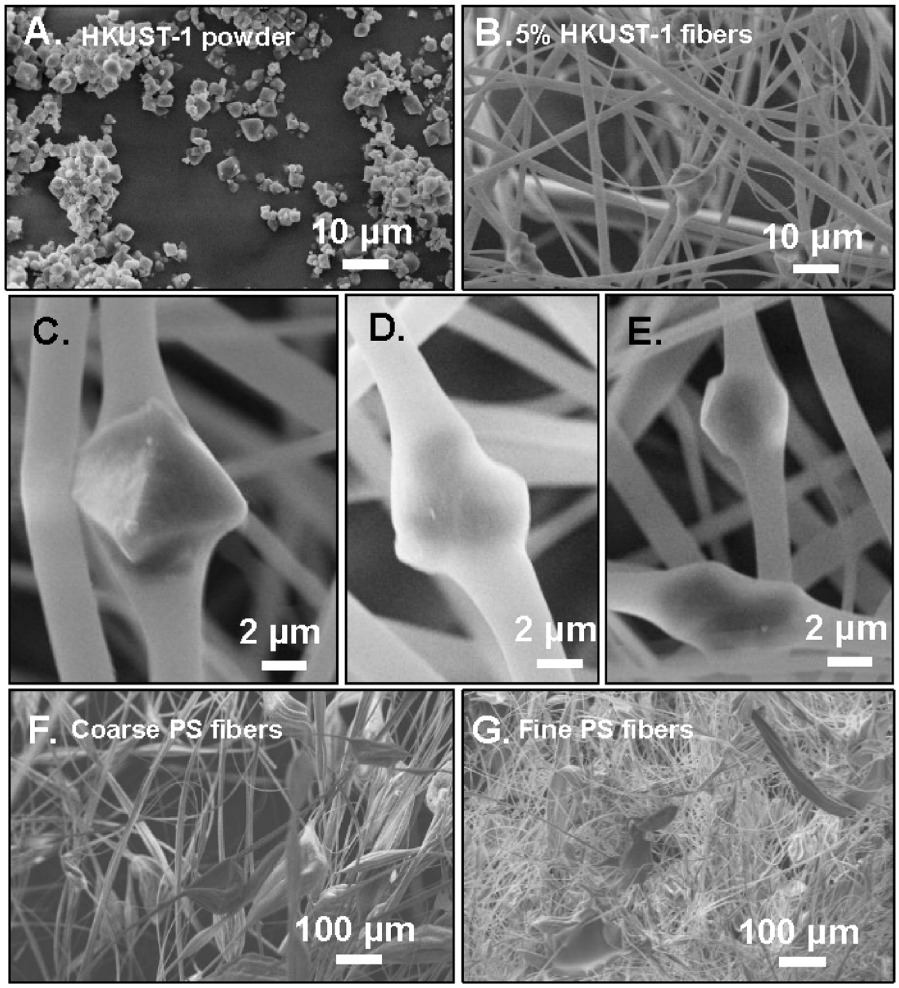

Fig. 4. SEM images of (A) HKUST-1 powder, (B) HKUST-1 embedded PS fibers, (C–E) higher magnifications of HKUST-1 embedded PS fibers, (F) coarse pure polystyrene fibers, and (G) fine pure polystyrene fibers.

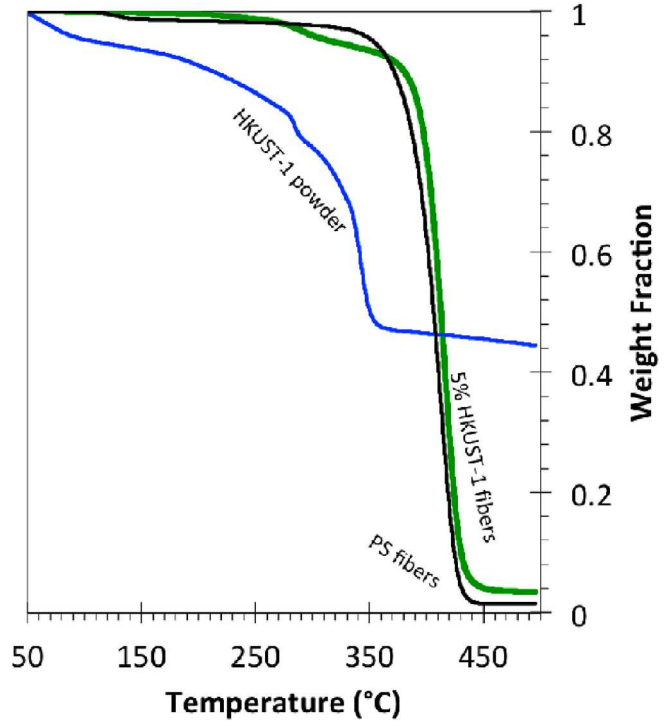

Fig. 5. Thermal Gravimetric Analysis of HKUST-1 powder (blue), PS fibers (black), and 5% HKUST-1 fibers (green). (For interpretation of the references to colour in this figure legend, the reader is referred to the Web version of this article.)

polystyrene as represented in the SEM images. The CO_2 isotherms show that the pure polystyrene samples take up nearly the same quantity of CO_2, demonstrating that CO_2 occurs primarily through an absorption mechanism since geometry does not appear to play a large role in uptake. This also suggests that CO_2 readily penetrates the fibers under these conditions. As a result of this, an estimated negligible influence of geometry is assumed. it may be expected that the uptake of CO_2 in the HKUST-1 embedded fibers may be approximated through a weighted average between the weight percent of polystyrene and the weight percentage of HKUST-1 through the equation:

$$Q_{Comp.} = wt\%_{PS} Q_{PS} + wt\%_{HKUST} Q_{HKUST} \quad (1)$$

where Q_{COMP} is the CO_2 uptake of the entire composite, Q_{PS} is the CO_2 uptake of the polystyrene component, Q_{HKUST} is the CO_2 uptake of the HKUST-1 component, $wt\%_{PS}$ is the weight percentage of the polystyrene component in the composite, and $wt\%_{HKUST}$ is the weight percentage of the HKUST-1 component in the composite.

Using the weight fractions interpolated through TGA experiments, the approximate quantity of CO_2 uptake expected for this material is 7.7 cm^3/g STP as calculated by EQ 1. This is in close agreement to the experimentally observed CO_2 uptake of 10 cm^3/g STP, demonstrating that the embedded HKUST-1 is readily available and negligibly damaged or blocked during the electrospinning process.

CO_2 isotherms were also collected for the HKUST-1 containing samples at different humidity exposure times as shown in Fig. 7. The CO_2 capacity of the HKUST-1 embedded fibers actually increases at 3 h, which is consistent with small water content loadings inside HKUST-1, where doubling of CO_2 capacity has been seen with 4% water loading [25]. However, this trend quickly turns and the capacity starts to drop. The estimated hydrolysis fraction of the HKUST-1 embedded fibers and HKUST-1 powder at different time-steps and near 100 kPa is shown in Fig. 8. Note that the data point at 3 h for the HKUST-1 embedded fibers was estimated based on the prediction that an increase in CO_2 uptake results in a hydrolysis degree of around 4%. All other data points for

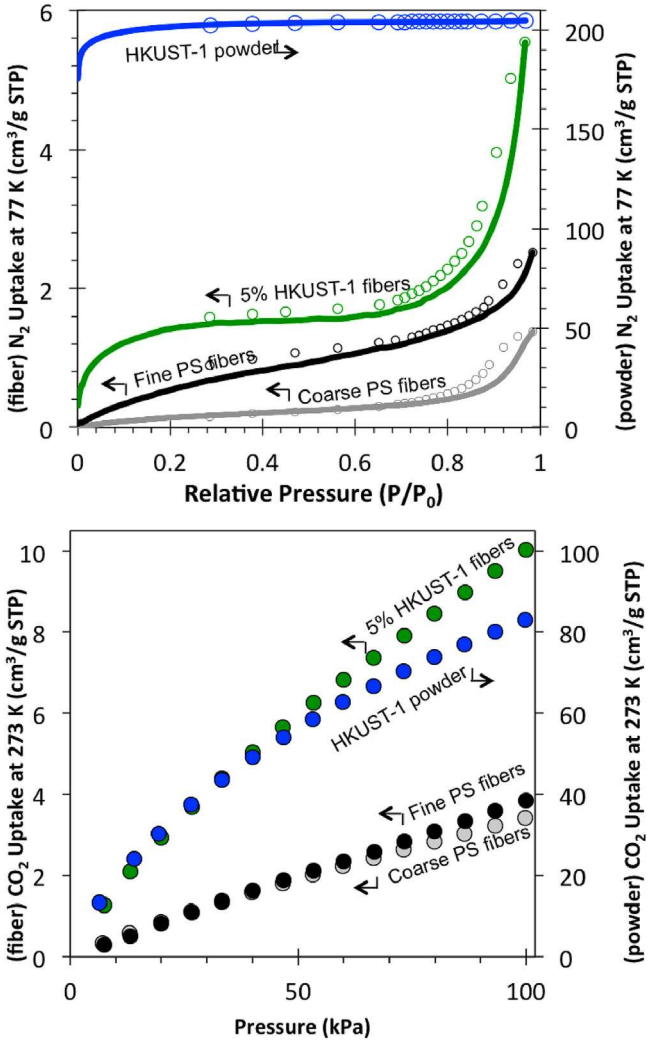

Fig. 6. N_2 isotherms at 77 K (top) and CO_2 isotherms at 273 K (bottom) for as-synthesized samples including HKUST-1 powder (blue), HKUST-1 embedded polystyrene fibers (green), fine pure polystyrene fibers (black) and coarse pure polystyrene fibers (grey). (For interpretation of the references to colour in this figure legend, the reader is referred to the Web version of this article.)

fractional hydrolysis are represented by the equation:

$$Fractional\ \ Hydrolysis = 1 - Q(t)/Q_0 \quad (2)$$

where $Q(t)$ is the CO_2 uptake capacity after t hours of hydrothermal treatment and Q_0 is the initial CO_2 uptake capacity. The pure HKUST-1 powder quickly loses CO_2 capacity. At 6 h of moisture exposure the sample is nearly completely destroyed. This appears to be in agreement with similar studies, where a similar study by Carné-Sánchez and coworkers test HKUST-1 hydrothermal stability at room temperature and 80% relative humidity, and show a 56% loss in N_2 uptake at 8 h [19]. The HKUST-1 embedded fibers show a slower hydrolysis rate than the pure HKUST-1 powder. This delayed loss confirms that these polystyrene fibers provide protection to the HKUST-1 particles by providing a barrier in which the moisture must overcome through a diffusion process before hydrolysis can occur.

SEM images of each material after 48h of high-temperature humidity exposure are shown in Fig. 9. From these images, it is clear that both materials were destroyed after 48 h of hydrothermal treatment, which agrees with the CO_2 uptake experiments.

By using electrospun fibers instead of more traditional encapsulation techniques a thin polystyrene barrier is formed. This is vital to the accessibility of the HKUST-1 particles to CO_2 uptake. The coating

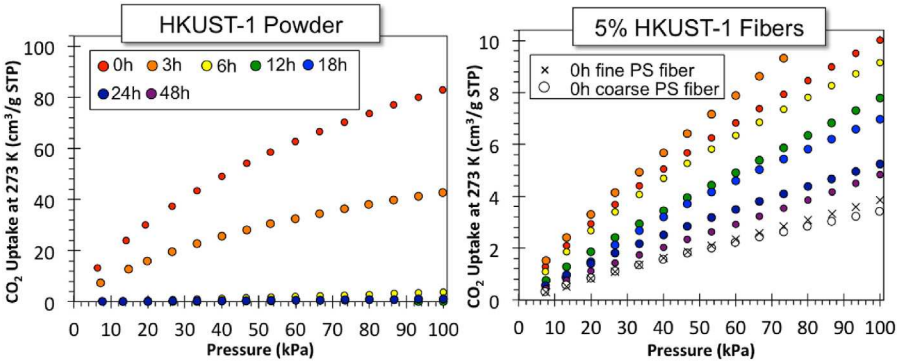

Fig. 7. CO_2 isotherms after varying degrees of hydrothermal exposure including 0 h (red), 3 h (orange), 6 h (yellow), 12 h (green), 18 h (blue), 24 h (indigo), and 48 h (violet). The figure on the left shows CO_2 isotherms for pure HKUST-1 powder, and the figure on the right shows CO_2 isotherms for HKUST-1 impregnated fibers, along with CO_2 isotherms for pure PS fibers with 0 h exposure. (For interpretation of the references to colour in this figure legend, the reader is referred to the Web version of this article.)

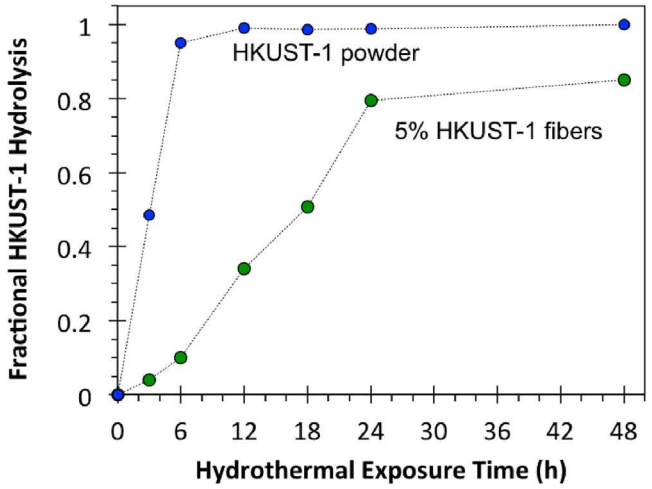

Fig. 8. Approximated Fractional HKUST-1 hydrolysis versus hydrothermal exposure time for HKUST-1 embedded polystyrene fibers (green) and HKUST-1 powder (blue). (For interpretation of the references to colour in this figure legend, the reader is referred to the Web version of this article.)

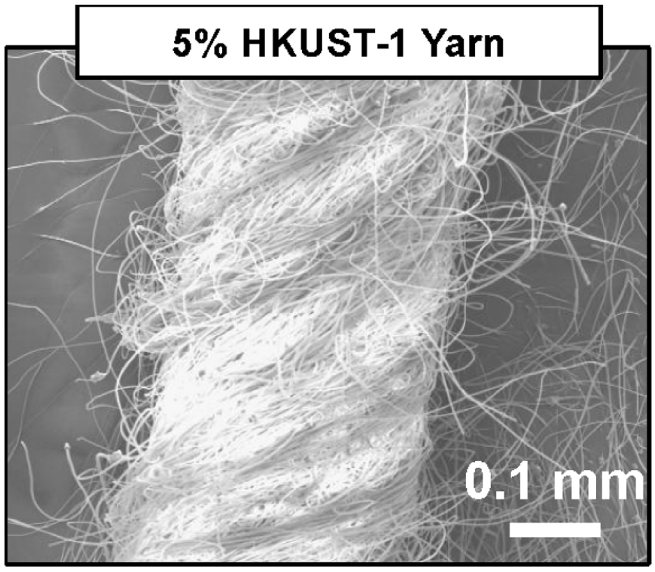

Fig. 10. SEM Image of HKUST-1 embedded fibers converted into yarn.

process realized during electrospinning appears to coat all particles in a thin barrier, which minimizes the diffusion barrier to CO_2 resulting in complete HKUST-1 accessibility. This uniform coating is not observed with more traditional techniques intended to make macroscopic particles. For example, Carné-Sánchez and coworkers suggested that when coating HKUST-1 in microspheres the particles near the center of the particles may not be accessible to CO_2 due to the thickness of the polymer coating [19]. Furthermore, as mentioned in the introduction, the use of fibers simultaneously provides a macroscopic dimension in addition to the nano-scopic coatings. This resulting macroscopic non-woven mat allows these materials to be directly processed using well established textile processes including the incorporation into filtration modules as non-woven mats or spun into yarn that could be further manufactured into fabrics. Therefore, this electrospinning technology allows for the formation of macroscopic MOF-textiles that may not be formed through other techniques. To demonstrate this potential, HKUST-1 embedded yarn is made with the 5% HKUST-1 fibers as shown in Fig. 10.

4. Conclusion

We present in this work the preparation and study of HKUST-1 particles encapsulated in polystyrene electrospun fibers for prolonged hydrothermal stability. MOFs have been encapsulated in hydrophobic polymer binders previously for hydrothermal stability, but drawbacks of these techniques include large variations in coatings and poor potential for handling and processing on the macroscale. This work shows

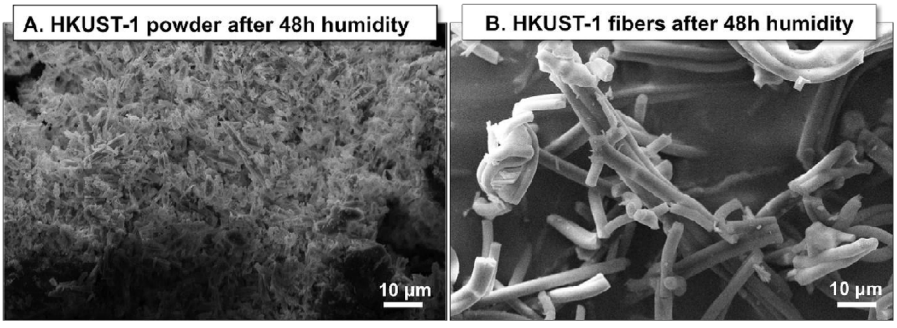

Fig. 9. SEM images of HKUST-1 powder and HKUST-1 embedded fibers after 48 h of hydrothermal treatment.

that the use of electrospun fibers may simultaneously solve both of these issues. SEM images show that the polystyrene fiber extends to wrap individual HKUST-1 particles in sub-micron coatings. It was demonstrated that tehse fibers are easily handled on the macroscale by converting the non-woven fibers into yarn. A loading of 5 wt% HKUST-1 in the fibers was found from TGA, and CO_2 sorption studies showed that the embedded HKUST-1 retained its CO_2 capacity. However, N2 isotherms did not show significant uptake inside of the embedded HKUST-1, which confirms that the polystyrene coating properly covered nearly all of the HKUST-1 particles. A hydrothermal time-study was performed and showed a significantly longer retention of CO_2 capacity in the HKUST-1 embedded in fibers versus pure HKUST-1 powder.

Acknowledgements

This research work was financially supported by Arizona State University and the National Science Foundation (Grant Number CBET-1748641). The authors gratefully acknowledge the use of the Leroy Eyring Center for Solid State Science at Arizona State University. Financial support by the National Natural Science Foundation of China (Project 21476082) is gratefully acknowledged.

References

[1] M.P. Suh, H.J. Park, T.K. Prasad, D.-W. Lim, Chem. Rev. 112 (2012) 782–835.
[2] J. Liu, P.K. Thallapally, B.P. McGrail, D.R. Brown, J. Liu, Chem. Soc. Rev. 41 (2012) 2308–2322.
[3] Y. Peng, V. Krungleviciute, I. Eryazici, J.T. Hupp, O.K. Farha, T. Yildirim, J. Am. Chem. Soc. 135 (2013) 11887–11894.
[4] P. Kumar, K. Vellingiri, K. Kim, R.J.C. Brown, M.J. Manos, Microporous Mesoporous Mater. 253 (2017) 251–265.
[5] A. Islas-jácome, E. González-zamora, Dalton Trans. 46 (2017) 9192–9200.
[6] A.W. Thornton, R. Babarao, A. Jain, F. Trousselet, F. Coudert, Dalton Trans. 45 (2016) 4352–4359.
[7] Y. Jiao, C.R. Morelock, N.C. Burtch, W.P. Moun, J.T. Hungerford, K.S. Walton, Ind. Eng. Chem. Res. 54 (2015) 12408–12414.
[8] H. Li, Z. Lin, X. Zhou, X. Wang, Y. Li, H. Wang, Z. Li, Chem. Eng. J. 307 (2017) 537–543.
[9] N. Qadir, S.A.M. Said, H.M. Bahaidarah, Microporous Mesoporous Mater. 201 (2015) 61–90.
[10] K.C. Jayachandrababu, D.S. Sholl, S. Nair, J. Am. Chem. Soc. 139 (2017) 5906–5915.
[11] Y. Zhao, L. Liu, W. Zhang, C. Sue, Q. Li, (2009) 13356–13380.
[12] X. Qian, F. Sun, J. Sun, H. Wu, F. Xiao, X. Wu, G. Zhu, Nanoscale 9 (2017) 2003–2008.
[13] S.J. Yang, C.R. Park, Adv. Mater. 24 (2012) 4010–4013.
[14] D. Desantis, J.A. Mason, B.D. James, C. Houchins, R. Long, M. Veenstra, Energy Fuels (2017) 2024–2032.
[15] M.R. Armstrong, C. Balzer, B. Shan, B. Mu, Langmuir 33 (2017) 9066–9072.
[16] B.R. Pimentel, A.W. Fultz, K.V. Presnell, R.P. Lively, Ind. Eng. Chem. Res. 56 (2017) 5070–5077.
[17] R.P. Lively, D.P. Leta, B.A. Derites, R.R. Chance, W.J. Koros, Chem. Eng. J. 171 (2011) 801–810.
[18] D. Mustafa, E. Breynaert, S.R. Bajpe, J. a Martens, C.E. a Kirschhock, Chem. Commun. 47 (2011) 8037–8039.
[19] A. Carné-Sánchez, K.C. Stylianou, C. Carbonell, M. Naderi, I. Imaz, D. Maspoch, Adv. Mater. 27 (2015) 869–873.
[20] M.R. Armstrong, S. Senthilnathan, C.J. Balzer, B. Shan, L. Chen, B. Mu, Ultrason. Sonochem. 34 (2017) 365–370.
[21] K. Yuriar-Arredondo, M.R. Armstrong, B. Shan, W. Zeng, W. Xu, H. Jiang, B. Mu, J. Membr. Sci. 546 (2018) 158–164.
[22] C. Balzer, M.R. Armstrong, B. Shan, Y. Huang, J. Liu, B. Mu, Langmuir 34 (2018) 1340–1346.
[23] M.R. Armstrong, B. Shan, B. Mu, MRS Adv 2 (2017) 2457–2463.
[24] M.R. Armstrong, K.Y.Y. Arredondo, C.-Y. Liu, J.E. Stevens, A. Mayhob, B. Shan, S. Senthilnathan, C.J. Balzer, B. Mu, Ind. Eng. Chem. Res. 54 (2015) 12386–12392.
[25] S.A. Faheem, P. Jakubczak, J.J. Low, R.R. Willis, R.Q. Snurr, Chem. Mater. (2009) 1425–1430.